

THE UNIVERSITY OF WARWICK

Original citation:

Rajpalke, M. K., Linhart, W. M., Birkett, M., Yu, K. M., Alaria, J., Kopaczek, J., Kudrawiec, R., Jones, T. S. (Tim S.), Ashwin, M. J. and Veal, T. D.. (2014) High Bi content GaSbBi alloys. *Journal of Applied Physics*, Volume 116 (Number 4). Article number 043511.

Permanent WRAP url:

<http://wrap.warwick.ac.uk/68773>

Copyright and reuse:

The Warwick Research Archive Portal (WRAP) makes this work of researchers of the University of Warwick available open access under the following conditions.

This article is made available under the Creative Commons Attribution 3.0 (CC BY 3.0) license and may be reused according to the conditions of the license. For more details see: <http://creativecommons.org/licenses/by/3.0/>

A note on versions:

The version presented in WRAP is the published version, or, version of record, and may be cited as it appears here.

For more information, please contact the WRAP Team at: publications@warwick.ac.uk

warwick**publications**wrap

highlight your research

<http://wrap.warwick.ac.uk>

High Bi content GaSbBi alloys

M. K. Rajpalke,¹ W. M. Linhart,¹ M. Birkett,¹ K. M. Yu,² J. Alaria,¹ J. Kopaczek,³ R. Kudrawiec,³ T. S. Jones,⁴ M. J. Ashwin,^{4,a)} and T. D. Veal^{1,b)}

¹Stephenson Institute for Renewable Energy and Department of Physics, School of Physical Sciences, University of Liverpool, Liverpool L69 7ZF, United Kingdom

²Materials Sciences Division, Lawrence Berkeley National Laboratory, 1 Cyclotron Road, Berkeley, California 94720, USA

³Institute of Physics, Wrocław University of Technology, Wybrzeże Wyspiańskiego 27, 50-370 Wrocław, Poland

⁴Department of Chemistry, University of Warwick, Coventry CV4 7AL, United Kingdom

(Received 14 March 2014; accepted 13 July 2014; published online 25 July 2014)

The epitaxial growth, structural, and optical properties of GaSb_{1-x}Bi_x alloys have been investigated. The Bi incorporation into GaSb is varied in the range $0 < x \leq 9.6\%$ by varying the growth rate ($0.31\text{--}1.33 \mu\text{m h}^{-1}$) at two growth temperatures (250 and 275 °C). The Bi content is inversely proportional to the growth rate, but with higher Bi contents achieved at 250 than at 275 °C. A maximum Bi content of $x=9.6\%$ is achieved with the Bi greater than 99% substitutional. Extrapolating the linear variation of lattice parameter with Bi content in the GaSbBi films enabled a zinc blende GaBi lattice parameter to be estimated of 6.272 Å. The band gap at 300 K of the GaSbBi epitaxial layers decreases linearly with increasing Bi content down to $410 \pm 40 \text{ meV}$ ($3 \mu\text{m}$) for $x=9.6\%$, corresponding to a reduction of $\sim 35 \text{ meV}/\% \text{Bi}$. Photoluminescence indicates a band gap of $490 \pm 5 \text{ meV}$ at 15 K for $x=9.6\%$. © 2014 Author(s). All article content, except where otherwise noted, is licensed under a Creative Commons Attribution 3.0 Unported License. [<http://dx.doi.org/10.1063/1.4891217>]

In recent years, dilute Bi containing III–V alloys have attracted great attention, particularly due to their properties of band gap reduction and enhanced spin-orbit coupling compared with the host material.^{1–3} Such properties make them suitable for optoelectronics device applications operating in the near- and mid-infrared ranges. A GaSb alloy with a few percent of Bi incorporated is a strong candidate for this purpose. However, very few studies of the growth of GaSbBi alloys have been reported. The earliest reports on GaSbBi alloys show very low Bi incorporation up to 0.8% (Refs. 4 and 5), unintentional As incorporation from the residual As in the growth chamber⁶ and lattice contraction compared with GaSb rather than the expected expansion.⁴ Band gap reduction of $\sim 40 \text{ meV}/\% \text{Bi}$ was estimated from photoluminescence (PL) results.⁵ Recently, there has been an attempt to grow GaSbBi alloys with high Bi content. These alloys show very large Sb/Bi droplets on the surface and unintentional arsenic incorporation in excess of 9%.⁶ Our earlier report on temperature-dependent growth shows Bi incorporation of up to 5% in GaSbBi alloys and absorption and photoreflectance spectroscopies indicate band gap reduction over this Bi-content range of $\sim 30\text{--}36 \text{ meV}/\% \text{Bi}$.^{7,8} However, the effects of growth rate on Bi incorporation in GaSbBi alloys have not been explored. It is crucial to understand and control the Bi incorporation in GaSbBi alloys in order to realise their potential for mid-infrared device applications.

Indeed, the molecular-beam epitaxy (MBE) growth of the more widely studied alloy GaAsBi has been beset by the issues of the dependence of Bi incorporation on growth

conditions^{9,10} and Ga, Ga-Bi, and Bi surface droplet formation.^{10,11} It has been found that the Bi incorporation requires low growth temperatures. Since such low temperatures suppress the desorption of group V species, near-stoichiometric growth conditions are required. This approach has led to highly crystalline GaAsBi films with up to 12% and 22% Bi being obtained by different groups.^{10,12} Arsenic-rich growth conditions produce droplet free surfaces, within 10% of stoichiometric conditions gives Ga droplets, and Ga-rich conditions lead to Ga-Bi droplets. It was suggested that the observed growth rate-dependence of the droplet formation can be attributed to the growth rate-dependence of the so-called stoichiometry threshold, the transition from group V-rich to group III-rich conditions. Moreover, it was proposed that this phenomenon is likely to occur in the MBE growth of a wide range of highly mismatched alloys that require near-stoichiometry growth conditions, including GaSbBi.¹¹

In this paper, the control of Bi content in GaSbBi alloys is demonstrated by varying the growth rate, enabling films with Bi contents of up to 9.6% to be produced. The incorporation of up to 9.6% Bi was achieved while maintaining greater than 99% substitutionality of the Bi. High resolution x-ray diffraction (HRXRD) and Rutherford backscattering spectroscopy (RBS) were used to study the Bi incorporation and the distribution of elements in the GaSbBi epilayers. The optical properties of GaSbBi alloys have been studied at room temperature using absorption spectroscopy and modeling that incorporates both the virtual crystal approximation (VCA) and valence band anticrossing (VBAC).

The GaSbBi epilayers were grown on undoped GaSb(001) substrates by solid-source MBE. The sources and substrate preparation procedure are described elsewhere.⁷ A

^{a)}Electronic mail: M.J.Ashwin@warwick.ac.uk

^{b)}Electronic mail: T.Veal@liverpool.ac.uk



GaSb buffer layer of 100 nm thickness was grown at 500 °C and substrates were cooled to the required temperature. The Ga cell temperature was adjusted for the required growth rate. The Bi beam equivalent pressure flux was then set to approximately 3.3×10^8 mbar using the beam monitoring ion gauge. The substrate temperature was measured by thermocouple calibrated by pyrometer measurements. The samples were grown under nominally slightly group V-rich conditions using growth rates in the range $0.31\text{--}1.33 \mu\text{m h}^{-1}$, at two different fixed growth temperatures of 250 and 275 °C. The film thicknesses were determined by RBS and confirmed by HRXRD measurement and were all in the range 320–375 nm.

The structural characterization was carried out using RBS with 3.72 MeV He^{2+} ions and by HRXRD using a Philips X'Pert diffractometer equipped with a Cu $K\alpha_1$ x-ray source ($\lambda = 0.15406$ nm). The surface morphology of GaSbBi alloys was investigated by JEOL JSM-7001 F field emission scanning electron microscopy (SEM). Transmittance measurements were carried out using a Bruker Vertex 70 V Fourier-transform infrared spectrometer, using a liquid nitrogen-cooled HgCdTe detector. For PL measurements, a single grating 0.3 meter focal-length monochromator and a thermoelectrically cooled InGaAs pin photodiode were used to disperse and detect the PL signal. A semiconductor laser (660 nm line and 40 mW) was used as the excitation source. The laser beam was focused onto the sample to a diameter of 0.1 mm and the power of the laser beam was tuned using a neutral density filter. Phase sensitive detection of the PL signal was accomplished using a lock-in amplifier.

As the lattice constant of zinc blende GaBi is unknown experimentally, the Bi content of GaSbBi films cannot reliably be obtained from the lattice constant by applying Vegard's law. This method has been used in some studies of GaAsBi alloys with a theoretically determined GaBi lattice parameter, but here, in common with other GaAsBi studies (for example, Ref. 13), the Bi fraction in the GaSbBi films was measured by RBS. Fig. 1 shows the RBS Bi content as a

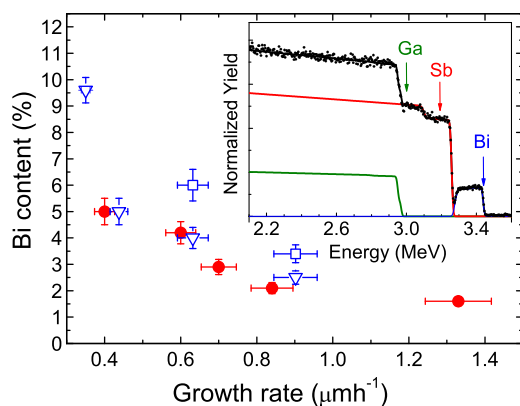


FIG. 1. The Bi content in $\text{GaSb}_{1-x}\text{Bi}_x$ epilayers as a function of growth rate at fixed growth temperatures 250 °C (open triangles) and 275 °C (closed circles) and Bi flux. The Bi content for the top layer of two of the films grown at 250 °C is also shown (open squares). The inset contains the RBS data (points) from the film grown at 250 °C with the lowest growth rate. The green, red, blue, and black lines correspond to the Ga, Sb, Bi, and total simulated contributions to the spectrum.

function of growth rate. The inset of Fig. 1 shows the RBS spectrum of the sample grown at 250 °C with the lowest growth rate. The contributions from Ga, Sb, and Bi atoms have been simulated using the SIMNRA code.¹⁴ The simulation indicates that the anion sublattice of this film contains 9.6% Bi. RBS indicated that for all but two samples the Bi content is uniform through the film. In the two samples grown at 250 °C with the highest growth rates, RBS indicates the presence of a ~ 65 nm layer at the surface with higher Bi content than the rest of the film. The composition from RBS of these top layers is also shown in Fig. 1. The Bi content decreases as the growth rate increases, at fixed growth temperature. The Bi contents are higher for growth at 250 °C than at 275 °C. Channeling RBS measurements show that all the uniform Bi-content films are of high crystallinity with greater than 99% of Bi atoms on substitutional group V lattice sites.

Fig. 2 shows the HRXRD ω -2 θ scans of GaSbBi samples with Bi content 1.6% and 4.2% grown at 275 °C with growth rate 1.33 and $0.60 \mu\text{m h}^{-1}$, respectively. The out-of-plane lattice dilation was confirmed by the lower Bragg angle peak for the GaSbBi film than that corresponding to the substrate. Lattice dilation has previously been observed in GaSbBi films with low Bi content ($<1\%$) grown by liquid phase epitaxy,⁵ and for up to 5% Bi in our previous temperature-dependent MBE growth.⁷ The earlier report on MBE grown GaSbBi shows lattice contraction and was explained in terms of group V vacancies.⁴ The diffraction peak from GaSbBi epilayers shifts towards lower angle with a decrease in the growth rate, indicating more Bi incorporation. The 004 reflections and the Pendellösung fringes were modeled by dynamical simulations. The lattice constant and the layer thickness were determined from the simulation. The sample with 4.2% Bi is 320 nm-thick and so exhibits a slightly broader diffraction peak than the sample with 1.6% Bi, which is 355 nm-thick. Asymmetric 115 reciprocal space

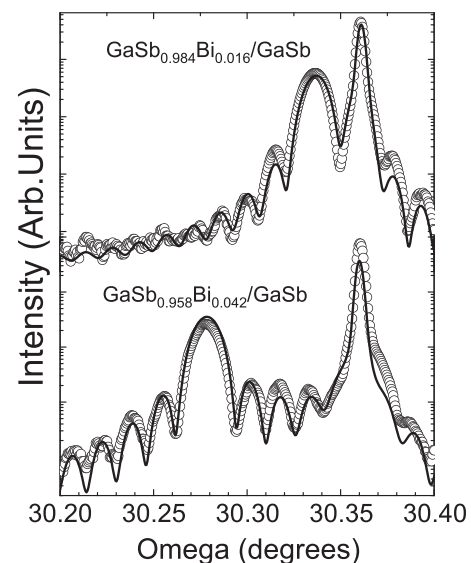


FIG. 2. HRXRD scans of the 004 Bragg reflection of GaSbBi films on GaSb(001) substrates. ω -2 θ scans of GaSbBi samples with Bi contents of 1.6 and 4.2% and film thicknesses of 355 and 320 nm, respectively, as determined from the simulations (solid lines).

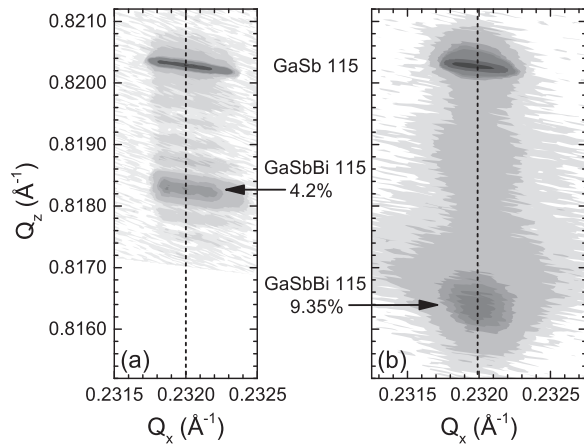


FIG. 3. Reciprocal space maps around the 115 reflections of GaSb and GaSbBi with Bi contents of 4.2% and 9.35%. Alignment of the GaSb and GaSbBi peaks along Q_x indicates that the films are not relaxed, that is, they are fully strained.

maps (RSM) were performed to study the strain state of the epilayers. Fig. 3 shows HRXRD RSMs around the 115 reflections of the GaSb substrate and the GaSbBi films with Bi contents of 4.2% and 9.35%. The asymmetric maps reveal that the $\text{GaSb}_{1-x}\text{Bi}_x$ films are completely strained to the GaSb in-plane lattice constant. The presence of Pendellösung interference fringes for the 4.2% Bi sample also indicates that the interfaces are smooth and the composition is uniform. The fringes are not clearly visible for the 9.35% Bi sample.

The lattice constant determined from the XRD is plotted in Fig. 4 as a function of the Bi content from RBS measurements. The lattice constants are for hypothetical free standing films, which are obtained by correcting the XRD data for the tetragonal distortion of the GaSbBi using the elastic constants of GaSb.^{7,15,16} The lattice parameters for growth rate dependent films (grown at 250 and 275 °C) show a linear trend with the Bi concentration in accordance with Vegard's law. The data points from the previous growth temperature dependent films have also been plotted. If this linear trend is extrapolated to 100% Bi, the lattice parameter corresponding to zinc blende GaBi is $6.272 \pm 0.005 \text{ \AA}$, somewhat smaller

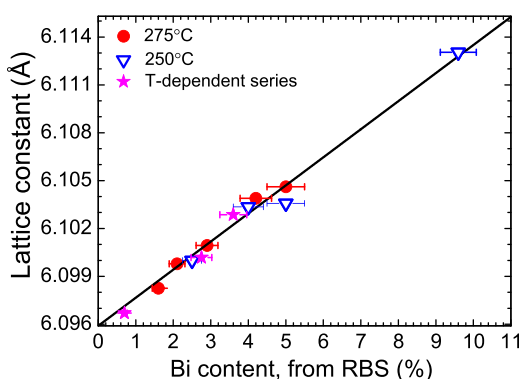


FIG. 4. Lattice parameters of growth rate dependent GaSbBi samples derived from HRXRD measurements by taking into account the tetragonal distortion of the pseudomorphic films plotted as a function of the Bi content from RBS. The lattice constant of growth temperature dependent samples has been plotted from Ref. 7.

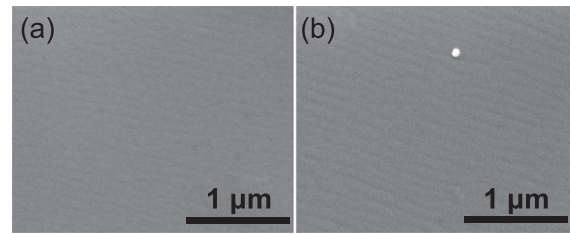


FIG. 5. SEM images of the samples containing (a) 4.2 and (b) 9.35% Bi.

than, but within the error range of, the value of $6.33 \pm 0.06 \text{ \AA}$ obtained from extrapolating the linear fit to RBS and XRD data from GaAsBi with up to 3.1% Bi.¹³

The surface morphology of the GaSbBi films was studied using SEM. Figure 5 shows the SEM image of the GaSbBi samples with 4.2% and 9.35% Bi incorporation. The images show smooth surfaces almost free of Ga, Bi, and Ga-Bi droplets and are typical of many of the films. A few Bi droplets are visible in the SEM images of the very lowest growth rate samples such as the one in the image of the 9.35% Bi sample shown in Fig. 5. Some films have surface Ga droplets present as observed by SEM and energy dispersive x-ray spectroscopy. By analogy with the previous results for GaAsBi,¹¹ this indicates that the growth conditions are group V-rich for the case of smooth surfaces and very close to stoichiometric when surface Ga droplets are observed.

The incorporation of Bi in GaSb is shown in Fig. 6 as a function of growth rate at growth temperatures of 250 and 275 °C. At both temperatures, the Bi content decreases with increasing growth rate. From the inset of Fig. 6, it can be seen that, at 275 °C, the incorporation of Bi is proportional to the inverse growth rate. The error bars in Fig. 6 reflect the uncertainties in the measurements of the Bi content and film thickness and do not include other uncertainties such as small temperature variations or small fluctuations in the V:III ratio.

The growth rate dependent Bi incorporation in GaSb has been modeled using the kinetic approach as described for Mg doping of GaAs by Wood *et al.*¹⁷ and N incorporation in both GaAs by Pan *et al.*¹⁸ and Ga(In)Sb by Ashwin

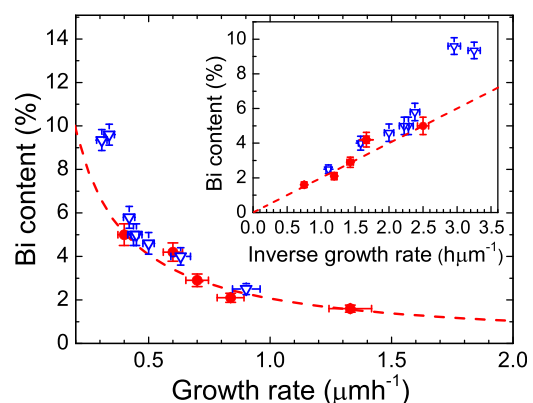


FIG. 6. Growth rate-dependence of the Bi content in GaSbBi films at fixed growth temperatures of 250 °C (open triangles) and 275 °C (closed circles) and fixed Bi flux. The dashed line is the calculated dependency from kinetic modeling for 275 °C. The Bi content as a function of inverse growth rate is plotted in the inset.

et al.^{16,19,20} The dashed line through the 275 °C data points in Fig. 6 corresponds to an energy barrier for Bi desorption of 1.75 eV and a characteristic surface residence lifetime of Bi atoms of 6.5 μ s. These are the same values as used previously to reproduce the temperature dependence of Bi incorporation in GaSbBi.⁷ A surface binding energy of 1.8 eV for Bi on GaAs has previously been reported.²¹ For comparison, the reported energy barriers for non-incorporation or desorption of N from GaSb and GaAs are 2.0 and 2.1 eV, respectively, and the surface residence lifetime of N was found to be 5 μ s for both GaSb and GaAs.^{18,20} The lower energy barrier for desorption of Bi than N is consistent with lower growth temperatures being required for Bi incorporation in GaSbBi than for N incorporation in GaSb and GaAs.

The growth behavior at 250 °C is more complicated; this is because of the presence of \sim 65 nm-thick “top” layers at the surface of two of the GaSbBi films with higher Bi content (6.0% and 3.4%) compared with the Bi content in the underlying 270 nm-thick “main” layers (4.0% and 2.5%) (see Fig. 1). While the main layers and the 5% Bi film follow a very similar inverse growth rate dependence to the samples grown at 275 °C, the samples with 9.35% and 9.6% Bi have Bi contents in excess of what is expected from inverse growth rate dependence. The growth behavior at 250 °C warrants further investigation; but at this stage, it seems that at the lowest growth rates there is an additional complication to the Bi incorporation that is not included in the simple kinetic model. Additionally, the indication from RBS that there is a transition between the main layer and the higher Bi content top layer in two of the films suggests the possibility of a change in growth mode, which occurs after several hundred nanometers of GaSbBi have been grown. It is unclear why there is this apparent change but there is a delicate balance to be maintained between the growth temperature, V:III ratio and Bi flux during growth. The growth of a high Bi content layer may be related to a change in the temperature of the growth surface (while the thermocouple reading remains constant), resulting from the growth of a narrow band gap material on a wider band gap substrate. Another possibility relates to the known surfactant behaviour of Bi whereby the buildup of Bi on the surface during growth leads to a change in the growth mode and hence to change in the incorporation of Bi.^{9–11}

Transmittance measurements were carried out at room temperature on the samples with uniform Bi content to determine the optical properties of the growth rate dependent GaSbBi samples as a function of Bi content. The absorption coefficient, α , was calculated from the transmittance data using Eq. (2) in Ref. 22. The transmission data from each sample was divided by the transmission from a GaSb substrate so that the remaining signal corresponds to transmission through a \sim 340-nm thick GaSbBi layer. The derived absorption spectra are shown in Fig. 7. (The peak at \sim 0.4 eV in the absorption spectrum of the sample with 9.6% Bi is due to water absorption and the water content of the residual vacuum being different when the sample and background spectra were collected.) The absorption edge red shifts with increasing Bi content. The absorption edge decreases in energy to 410 ± 40 meV as the Bi content is increased to $x = 9.6\%$, which corresponds to a wavelength of 3.0 μ m. As

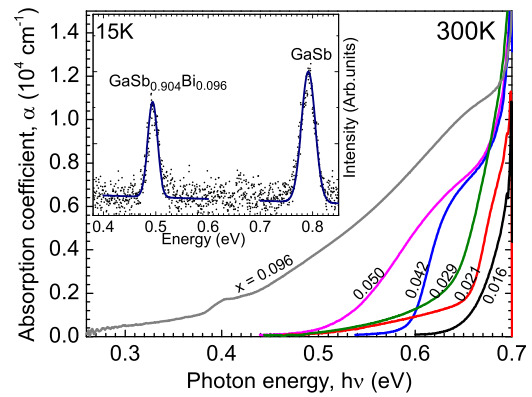


FIG. 7. The absorption spectra recorded at 300 K for growth rate dependent GaSb_{1-x}Bi_x films at a growth temperature of 275 °C and the sample with 9.6% Bi grown at 250 °C. The composition of each film is given in the figure. The inset shows a photoluminescence spectrum recorded at 15 K from the sample with 9.6% Bi. The peaks are fitted with a Gaussian lineshape to aid estimation of the peak position and as a guide to the eye.

the absorption spectrum of the 9.6% sample is relatively broad for accurate determination of the band gap, a PL spectrum has also been recorded at 15 K from this sample and is shown inset in Fig. 7. The peak at 790 meV is associated with bound exciton recombination in the GaSb buffer layer and substrate. The peak at 490 meV is attributed to band gap-related emission in the GaSb_{0.904}Bi_{0.096} layer. This assignment is based on a comprehensive PL study of GaSbBi with Bi content up to 4.2%.²³ Therefore, the band gap at 15 K of the 9.6% Bi film is found to be 490 ± 5 meV. This is consistent with the room temperature band gap determined from absorption of 410 ± 40 meV as photoreflectance data has previously indicated a \sim 70 meV change in band gap between 15 and 290 K.⁸

The absorption edge energies are plotted in Fig. 8. The dashed line shows the VCA band gap reduction, which deviates from the experimental data. This is based on conduction and valence band offsets between GaSb and GaBi of -2.83 eV and 0.03 eV, respectively, based on previously used valence band offsets between GaAs, GaSb, and GaBi

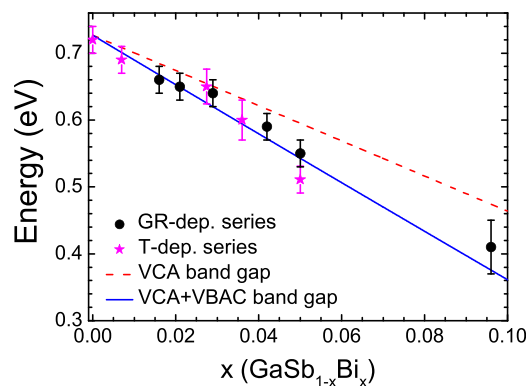


FIG. 8. The band gap versus Bi content determined from the absorption spectra in Fig. 7 (closed circles). The band gap of GaSb_{1-x}Bi_x calculated assuming the VCA variation of both the CBM and the VBM (dashed line) and by assuming the VCA variation of the CBM and VBAC between the valence bands and the Bi impurity level (solid line). The optical band gap of GaSb_{1-x}Bi_x films grown at different temperatures (stars) has been plotted together for comparison (data from Ref. 7).

(Ref. 24), the room temperature band gap of GaSb of 720 meV and the negative band gap of semi-metallic GaBi of -2.14 eV from recent hybrid functional density functional theory calculations.⁷ The VBAC model (solid line) was used to account for the additional band gap reduction. The observed band gap is well reproduced by the $12 \times 12 \mathbf{k} \cdot \mathbf{p}$ model described by Alberi *et al.* for GaAsSb and GaAsBi.²⁴ The band gap reduction is ~ 35 meV/%Bi and extends our earlier report on growth temperature dependent GaSbBi from up to 5% (Ref. 7) to as far as 9.6% Bi incorporation.

In conclusion, Bi contents in GaSbBi epilayers of up to 9.6% have been demonstrated by varying the growth rate. The GaSbBi alloys show droplet free smooth surfaces and high crystalline quality with greater than 99% of the incorporated Bi found to be substitutional on the group V sublattice. At 275 °C, the Bi incorporation is found to be inversely proportional to the growth rate, which has been reproduced by kinetic modeling. The growth behaviour at 250 °C is found to be more complicated. GaSbBi alloys are promising for mid-infrared applications with band gap energy reduction to ~ 410 meV, corresponding to a shift to a wavelength of $3.0 \mu\text{m}$, for 9.6% Bi incorporation.

The work at Liverpool and Warwick was supported by the University of Liverpool and the Engineering and Physical Sciences Research Council (EPSRC) under Grant Nos. EP/G004447/2 and EP/H021388/1 and the work at Wrocław by the NCN (Grant No. 2012/07/E/ST3/01742). RBS measurements performed at Lawrence Berkeley National Lab were supported by the Director, Office of Science, Office of Basic Energy Sciences, Materials Sciences and Engineering Division of the U.S. Department of Energy under Contract No. DE-AC02-05CH11231.

¹S. Francoeur, M.-J. Seong, A. Mascarenhas, S. Tixier, M. Adamczyk, and T. Tiedje, *Appl. Phys. Lett.* **82**, 3874 (2003).

²X. Lu, D. A. Beaton, R. B. Lewis, T. Tiedje, and Y. Zhang, *Appl. Phys. Lett.* **95**, 041903 (2009).

³B. Fluegel, S. Francoeur, A. Mascarenhas, S. Tixier, E. C. Young, and T. Tiedje, *Phys. Rev. Lett.* **97**, 067205 (2006).

⁴Y. Song, W. Shumin, I. S. Roy, P. Shi, and A. Hallen, *J. Vac. Sci. Technol. B* **30**, 02B114 (2012).

⁵S. K. Das, T. D. Das, S. Dhar, M. de la Mare, and A. Krier, *Infrared Phys. Technol.* **55**, 156 (2012).

⁶A. Duzik and J. M. Millunchick, *J. Cryst. Growth* **390**, 5 (2014).

⁷M. K. Rajpalke, W. M. Linhart, M. Birkett, K. M. Yu, D. O. Scanlon, J. Buckeridge, T. S. Jones, M. J. Ashwin, and T. D. Veal, *Appl. Phys. Lett.* **103**, 142106 (2013).

⁸J. Kopaczek, R. Kudrawiec, W. M. Linhart, M. K. Rajpalke, K. M. Yu, T. S. Jones, M. J. Ashwin, J. Misiewicz, and T. D. Veal, *Appl. Phys. Lett.* **103**, 261907 (2013).

⁹X. Lu, D. A. Beaton, R. B. Lewis, T. Tiedje, and M. B. Whitwick, *Appl. Phys. Lett.* **92**, 192110 (2008).

¹⁰A. J. Ptak, R. France, D. A. Beaton, K. Alberi, J. Simon, A. Mascarenhas, and C.-S. Jiang, *J. Cryst. Growth* **338**, 107 (2012).

¹¹G. Vardar, S. W. Paleg, M. V. Warren, M. Kang, S. Jeon, and R. S. Goldman, *Appl. Phys. Lett.* **102**, 042106 (2013).

¹²R. B. Lewis, M. Masnadi-Shirazi, and T. Tiedje, *Appl. Phys. Lett.* **101**, 082112 (2012).

¹³S. Tixier, M. Adamczyk, T. Tiedje, S. Francoeur, A. Mascarenhas, P. Wei, and F. Schiettekatte, *Appl. Phys. Lett.* **82**, 2245 (2003).

¹⁴L. Mayer, "SIMNRA, a simulation program for the analysis of NRA, RBS, and ERDA," in *Proceedings of the 15th International Conference on Application Accelerators in Research and Industry*, edited by J. L. Duggan and I. L. Morgan (AIP, NY, 1999), Vol. 475, p. 541.

¹⁵I. Vurgaftman, J. R. Meyer, and L. R. Ram-Mohan, *J. Appl. Phys.* **89**, 5815 (2001).

¹⁶M. J. Ashwin, R. J. H. Morris, D. Walker, P. A. Thomas, M. G. Dowsett, T. S. Jones, and T. D. Veal, *J. Phys. D: Appl. Phys.* **46**, 264003 (2013).

¹⁷C. E. C. Wood, D. Desimone, K. Singer, and G. W. Wicks, *J. Appl. Phys.* **53**, 4230 (1982).

¹⁸Z. Pan, L. H. Li, W. Zhang, Y. W. Lin, and R. H. Wu, *Appl. Phys. Lett.* **77**, 214 (2000).

¹⁹M. J. Ashwin, D. Walker, P. A. Thomas, T. S. Jones, and T. D. Veal, *J. Appl. Phys.* **113**, 033502 (2013).

²⁰M. J. Ashwin, T. D. Veal, J. J. Bomphrey, I. R. Dunn, D. Walker, P. A. Thomas, and T. S. Jones, *AIP Adv.* **1**, 032159 (2011).

²¹E. C. Young, S. Tixier, and T. Tiedje, *J. Cryst. Growth* **279**, 316 (2005).

²²C. Ghezzi, R. Magnanini, A. Parisini, B. Rotelli, L. Tarricone, A. Bosacchi, and S. Franchi, *Phys. Rev. B* **52**, 1463 (1995).

²³J. Kopaczek, R. Kudrawiec, W. M. Linhart, M. K. Rajpalke, T. S. Jones, M. J. Ashwin, and T. D. Veal, "Photoluminescence studies of GaSb_{1-x}Bi_x layers with $0 < x \leq 0.042$: Recombination between the conduction band and acceptor states versus the valence band," (unpublished).

²⁴K. Alberi, J. Wu, W. Walukiewicz, K. M. Yu, O. D. Dubon, P. S. Watkins, C. X. Wang, X. Liu, Y.-J. Cho, and J. Furdyna, *Phys. Rev. B* **75**, 045203 (2007).